Classification of Cognitive Ability of Healthy Elderly Individuals Using Resting-State Functional Connectivity Magnetic Resonance Imaging and An Extreme Learning Machine

Zekun Yang (✉ 598011294@qq.com)

Hebei University of Technology

Manling Ge

Hebei University of Technology

Abdelkader Nasreddine Belkacem

United Arab Emirates University

Xiaoxuan Fu

Harvard Medical School

Qirui Zhang

Nanjing University School of Medicine/General Hospital of Eastern Theater

Shenghua Chen

Hebei University of Technology

Chong Xie

Hebei University of Technology

Zibo Song

Hebei University of Technology

Chao Chen

Hebei University of Technology

Classification of Cognitive Ability of Healthy Elderly Individuals Using Resting-State Functional Connectivity Magnetic Resonance Imaging and An Extreme Learning Machine

Yang Zekun[a,b], Ge Manling[a,b], Abdelkader Nasreddine Belkacem[c], Fu Xiaoxuan[a,b,d], Zhang Qirui[e], Chen Shenghua[a,b*],   Xie Chong[a,b], Song Zibo[a,b], Chen Chao[a,b,f*]

[a]State Key Laboratory of Reliability and Intelligence of Electrical Equipment, Hebei University of Technology, Tianjin,300130, China

[b]Hebei Province Key Laboratory of Electromagnetic Field and Electrical Apparatus Reliability, Hebei University of Technology, Tianjin,300130, China

[c]Department of Computer and Network Engineering, College of Information Technology, United Arab Emirates University, Al Ain, 15551, UAE

[d]Athinoula A. Martinos Center for Biomedical Imaging, Department of Radiology, Massachusetts General Hospital, Harvard Medical School, Charlestown, Massachusetts, 02129, USA

[e]Department of Medical Imaging, Jinling Hospital, Nanjing University School of Medicine/General Hospital of Eastern Theater, Nanjing,210002, China

[f]Key Laboratory of Complex System Control Theory and Application, Tianjin University of Technology, Tianjin, 300003,China

[*]**Corresponding Author:**Chen Shenghua
8 #Guangrong Road, Hongqiao District, Hebei University of Technology,Tianjin300130, China

Email: chenshenghua@hebut.edu.cn

[*]**Equal corresponding Authors:**Chen Chao

391 #Binshui East Road, Xiqing District, Tianjin University of Technology,Tianjin300003, China

Email: cccovb@hotmail.com

Abbreviations[1]

---

[1] FC: Functional Connectivity; fMRI: functional Magnetic Resonance Imaging; rs-fMRI: resting-state functional Magnetic Resonance Imaging; fcMRI: resting-state functional connectivity Magnetic Resonance Imaging; GSP: Brain Genomics Superstructure Project; WM: White Matter; AAL: Automatic Anatomical Labeling; CDI: Connectome Distinctiveness Index; ROI: Regions Of Interest; ROC: Receiver Operating Characteristic; ELM: Extreme Learning Machine; CA: Classification Accuracy; EMCI: Early Mild Cognitive Impairment; LMCI: Late Mild Cognitive Impairment.

ABSTRACT

Purpose Quantitative determination of the correlation between cognitive ability and functional biomarkers in the elderly brain is essential. To identify biomarkers associated with cognitive performance in the elderly, this study combined an index model specific for resting-state functional connectivity (FC) magnetic resonance imaging (fcMRI) with a supervised machine learning method.

Methods Performance scores on conventional cognitive test batteries and MRI data were obtained for 98 healthy elderly individuals and 90 healthy youth from two public databases. Based on the test scores, the elderly cohort was categorized into two groups: excellent and poor. An fcMRI index model was constructed for each elderly individual to determine the relative differences in FC among brain regions compared with that in the youth cohort. Brain areas sensitive to test scores could then be identified using the fcMRI indexes. To confirm the effectiveness of constructed model, the fcMRI indexes of these brain areas were used as feature matrix inputs for training an extreme learning machine. Classification accuracy was then tested in separate groups and confirmed by N-fold cross-validation.

Results This learning study could effectively classify the cognitive status of healthy elderly individuals according to frontal lobe, temporal lobe, and parietal lobe FC values with a mean accuracy of 83.5%, which is substantially higher than that achieved using conventional correlation analysis.

Conclusion This fcMRI classification study may facilitate early detection of age-related cognitive decline as well as help reveal the underlying pathological mechanisms.

Keywords: index model, resting-state functional connectivity magnetic resonance imaging, cognitive test score, extreme learning machine, N-fold cross-validation

1. Introduction

The increase in the aging population in many countries has led to an increase in the prevalence of cognitive and physical impairments, necessitating research efforts to develop efficacious treatment strategies for improving the quality of life of the elderly. An age-related decline in cognitive abilities may be an early indicator of neurodegenerative and psychiatric disorders such as Alzheimer's disease[1]. The factors that affect cognitive ability may be diverse, such as cognitive load of exercise[2], etc. Therefore, cognitive evaluation of the elderly at an early stage and timely interventions will help reduce the rate of deterioration. Conventional cognitive tests designed, authorized, and measured by psychologists generally assess the cognitive abilities of elderly individuals [3-6]. However, comprehensive testing is time-consuming and complex and scoring can be subjective, which affect the accurate evaluation of cognitive functions of the elderly. In contrast, functional imaging methods such as positron emission computed tomography (PET) and functional magnetic resonance imaging (fMRI) utilizes advanced technology to provide objective measurements of cognitive functions [7,8]. Furthermore, fMRI evaluations can be conducted both during tasks engaging specific neural networks or in the resting state to provide an unbiased (task-independent) assessment of network activity [9,10].

Resting-state functional connectivity (FC) MRI (fcMRI) can reveal the FC of the whole brain by measuring the spatiotemporal correlations in regional brain activity established by Hebbian-like learning mechanisms [11-16]. In addition, fcMRI is noninvasive and objective, and in contrast to neuropsychiatric tests and task-dependent fMRI, can

be conducted quickly (in less than 15 min), thereby permitting larger-scale screening of elderly populations free of outcome variations conferred by different cognitive tasks and subject scoring criteria.

Several well-known fMRI-based consortium projects have supplied public fMRI datasets to estimate the FC, including the International Consortium for Brain Mapping established in 1992; the United States Human Connectome Project (http://www.humanconnectome.org/), which provided a stable brain function computing template; and the Brain Genomics Superstructure Project (GSP, http://dx.doi.org/10.7910/dvn/25833) established by Harvard Medical School in 2014. There are also large public databases combining various fMRI and psychometric test performance results (e.g., github.com/juanitacabral/LEiDA).

Previous studies have found that the youth exhibit an optimal network framework for language processing characterized by highly integrated local networks with strong FC and weaker FC between networks [17], whereas elderly individuals with reduced language comprehension demonstrate a sub-

optimal network structure characterized by stronger FC between networks [18]. However, these findings were derived from group-level analyses.

These fcMRI findings may help identify elderly individuals at risk of progressive cognitive impairment and thus facilitate timely intervention. At present, a combination of structural MRI imaging and machine learning is used to classify elderly individuals with cognitive impairment[19]. However, there are few models to identify quantitative regional fcMRI biomarkers sensitive to cognitive scores among healthy elderly individuals. Here a fcMRI index model specific to healthy elderly individuals is proposed based on a connectome dataset. The model uses the degree of fcMRI deviation between elderly individuals and a youth cohort to identify brain regions most sensitive to cognitive test performance scores. The ability of these fcMRI index values to accurately classify elderly individuals with intact or poor cognition was then tested using a machine learning model. The study flowchart is shown in Figure 1.
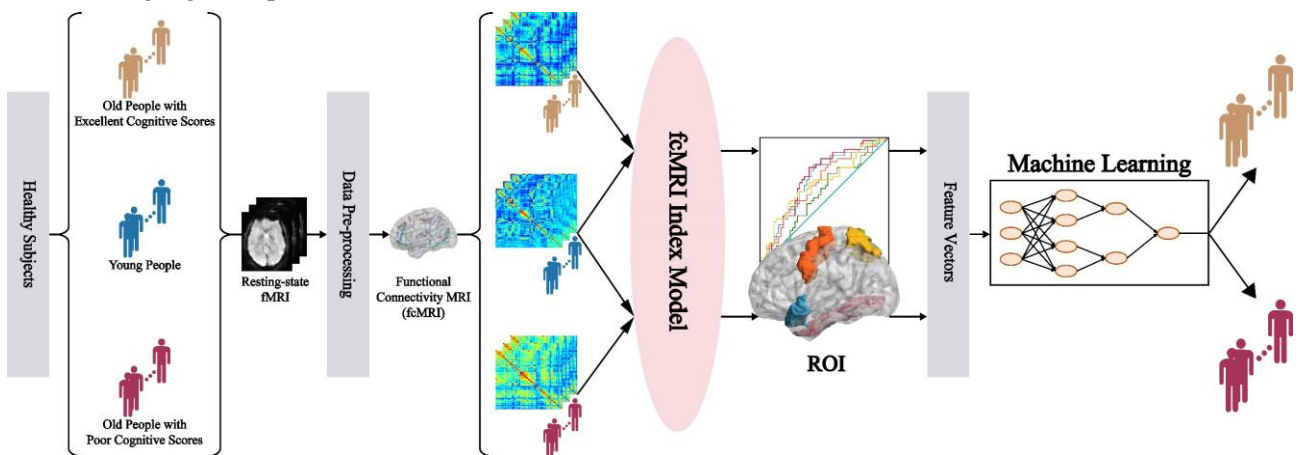

Fig. 1. Study flowchart

2. Material and methods

2.1. Experimental dataset

(1) Healthy elderly group

Elderly individuals were selected from a public dataset (github.com/juanitacabral/LEiDA) derived from a cohort study involving 1,051 healthy Portuguese elderly individuals aged >50 years who

were subjected to nine neuropsychological tests. The tests were approved by certified psychologists and were confirmed to evaluate two related dimensions of cognitive performance: memory-related and general performance functions-related, by principal component analysis. Cluster analysis based on the scores of these two dimensions and those of other related variables such as health status revealed four functional categories: C1 (excellent cognition) > C2 > C3 > C4 (poor cognition) [3]. The influences of other co-variables such as age and sex were eliminated by data pre-processing. Ninety-eight subjects were randomly selected from the C1 and C4 groups to undergo rs-fMRI scans: 55 subjects with excellent cognitive scores (excellent group) and 43 with poor cognitive scores (poor group). This study was performed in accordance with the Declaration of Helsinki (59th amend-ment) , and all subjects provided written informed consent [3].

(2) Healthy youth group

Ninety healthy youth aged 18 – 35 years were selected from >1500 subjects in the GSP database (http://doi.org/10.7910/dvn/25833). The dataset for each participant in the GSP database includes 1) basic demographic and health information before and after MRI scans, 2) structural and functional MRI scans, 3) results from saliva samples taken before and after scans, and 4) network-based behavioral, cognitive, and personality assessments. Before scanning, all neurological functions, psychological evaluations, and language comprehension scores were confirmed to be above the population median. Subjects with mental illness or a history of mental illness were excluded. This study was performed in accordance with the Declaration of Helsinki (59th amend-ment) , and all subjects provided written informed consent [20].

2.2. Data pre-processing

All rs-fMRI data were pre-processed in the following steps using the FMRIB software library (FSL V5.07; http://fsl.fmrib.ox.ac.uk/fsl)[21]. (1) The first five acquisition time series were removed to stabilize the signal. (2) Slice timing correction was performed. (3) MCFLIRT software was used to perform rigid body alignment motion correction [22]. (4) The brain extraction tool was used for skull peeling [23]. (5) Nonlinear normalization through continuous rigid body registration was performed. FLIRT software was employed to obtain the structure from the original space, and nonlinear registration was performed in Montreal Neurological Institute standard space, followed by re-sampling to an isotropic voxel size of 2 mm^3. (6) Linear regression was conducted to remove motion parameters, mean cerebrospinal fluid signals, and white matter (WM) signals. (7) Finally, band-pass time filtering of regression residuals (0.01–0.08 Hz) was conducted. When SPM software was used for FC analysis, co-variables in fcMRI data needed to be removed, such as head movement parameters, whole-brain signals, WM signals, cerebrospinal fluid signals, and other relevant co-variables, e.g., age, sex, etc.

All rs-fMRI data were acquired using a 1.5 T Siemens Magnetom Avanto 12 channel head coil scanner and a bold oxygen level-dependent (BOLD) echo planar imaging sequence, yielding 3.5 × 3.5 × 3.5 mm voxels for the elderly group and 3 × 3 × 3 mm voxels for the youth group. Voxels were then assigned to 116 brain regions according to the automatic anatomical labeling (AAL) atlas. The mean BOLD signal of each voxel belonging to a given AAL region was subjected to post-processing analysis [24].

2.3. Post-processing

2.3.1. fcMRI

Traditionally, the Pearson correlation coefficient is used to quantify the degree of dependence between regional brain activity patterns (time series) assuming a static BOLD signal and inclusion of all time series for fcMRI estimation [25]. A correlation coefficient of >0 implies that excitation in one area is associated with excitation in another (and vice versa) [24], whereas a coefficient of <0 implies that excitation in one region is associated with inhibition in another. A coefficient of 1 implies self-correlation, whereas a coefficient of 0 implies no correlation between two brain areas. The absolute value of the coefficient represents the degree of correlation. A one-sided t-test was performed to assess the significance of the correlation, with a *p*-value of ≤ 5% considered significant for all paired regions. Because each subject's brain was divided into 116 functional regions, this analysis yielded a 116 × 116 matrix of correlations, and the fcMRI strength was derived for a single mean value at each brain region. A toolbox for surfaces, nodes, and edges in BrainNet Viewer software was employed to display fcMRI networks [26].

2.3.2. The fcMRI index model

To identify functional neuroimaging markers with sensitivity to cognitive test scores, a fcMRI index model was constructed from the differences in regional fcMRI values between each elderly individual and the youth cohort. In the model, the regional fcMRI difference between areas "s" and "i" in the elderly brain relative to areas "i" and "p" in the youth brain is expressed as a connectome distinctiveness index (*CDI*).

$$CDI_{s,i} = \frac{1}{N-1}\sum_{p=1,p\neq s}^{N}\left(1 - corr\left(f_{s,i}, f_{p,i}\right)\right)$$
(1)

where $f_{s,i}$ is the fcMRI vector between the i-th area

and the s-th area in the elderly brain, $f_{p,i}$ is the fcMRI vector between the i-th area and the p-th area in the youth brain, N is the number of healthy youth, and $CDI_{s,i}$ is the fcMRI index between the s-th area and the i-th area in the healthy elderly brain.

The CDI value for each region pair in the elderly brain was estimated relative to that in the youth brain; thus, a total of 98 × 116 CDI matrices were derived for the elderly brain and a total of 90 × 116 CDI matrices for the youth brain.

The distribution of CDI values in the youth brain was evaluated using the equations

$$mean\_CDI_i = \frac{1}{N}\sum_{s=1}^{N} CDI_{s,i}$$
(2)

and

$$std\_CDI_i = sqrt\left(\frac{1}{N-1}\sum_{s=1}^{N}\left(CDI_{s,i} - mean\_CDI_i\right)^2\right)$$
(3)

where $mean\_CDI_i$ represents the average CDI for N healthy youth (N = 90) and std_CDI_i is the standard deviation of CDI at the *i*-th brain area.

After averaging the 90 × 116 CDI matrices for all youth, a 1 × 116 CDI matrix denoted as $mean\_CDI\_nc$ was formed, which represented the distribution of CDI values across brain areas. The standard deviation of CDI is denoted as std_CDI_nc, which is a 1 × 116 matrix representing the degree of CDI dispersion among individuals in a group.

Relative to the *CDI* distribution at the *i*-th brain area in all youth, the CDI value at the *i*-th brain area of the *s*-th elderly individual is defined as

$$Z_{s,i} = \frac{1}{std\_CDI_i}\left(CDI_{s,i} - mean\_CDI_i\right)$$
(4)

This index model can objectively estimate the fcMRI deviation from healthy youth for each AAL-labeled brain region, with higher index values

indicating a greater degree of deviation in an elderly individual. As 98 healthy elderly individuals were examined, 98 × 116 index matrices were formed.

2.3.3．*Identification of functional biomarker regions by fcMRI between the elderly and youth brain*

First, the fcMRI indexes for each brain area were averaged across subjects within each age group. The differences in indexes between the 116 brain regions were calculated using equation (5), and those regions with greatest differences were defined as regions of interest (ROIs).

$$Index\_difference = \left| \frac{1}{n}\sum_{i=1}^{n} Z_{s,i-excelent} \sum_{i=1}^{n} Z_{s,i-poor} \right| \quad (5)$$

Between-group differences in fcMRI indexes were evaluated using independent samples t-tests (significance level, α = 5%), and receiver operating characteristic (ROC) curves were constructed using SPSS (IBM SPSS Statistics 21; USA). The BrainNet Viewer toolbox was also employed to highlight functional biomarker regions on a whole-brain template image [24].

2.4．**Extreme learning machine (ELM)**

2.4.1．*Feature vectors*

The fcMRI indexes in brain areas identified as functional biomarkers (ROIs) were then considered as feature vectors for the ELM input layer, with those from the poor cognition group labeled as 1 and those from the excellent cognition group labeled as 2.

2.4.2．*ELM model*

Compared with conventional artificial neural network models, an advantage of ELMs is that the model can randomly generate both the connection weights between the input layer and the hidden layer and the threshold values of neurons in the hidden layer. For training, ELM requires only a known number of neurons in the hidden layer for it to converge on a unique optimal solution. A flowchart of ELM construction, training, and testing is shown in Figure 2.
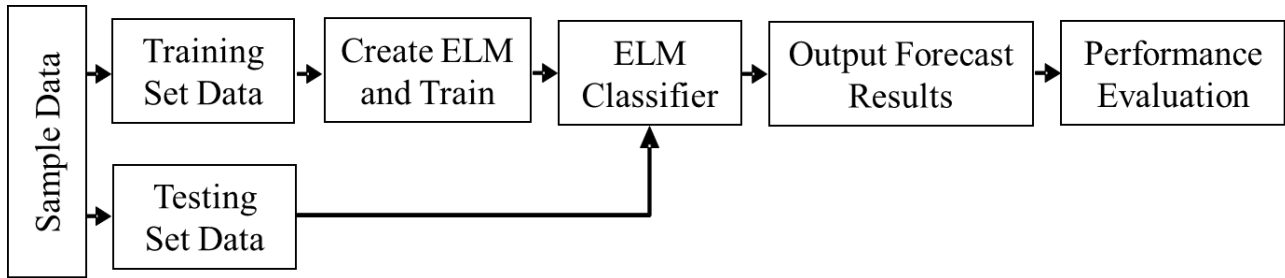

Fig. 2. Flowchart of extreme learning machine (ELM) classifier

The main steps of the ELM model are as follows. (1) Training and testing datasets of sufficient size for ELM generalization and prediction performance were established. (2) The ELM was constructed and trained using the "elmtrain" function. A suitable number of hidden neurons was set for best performance. (3) Simulation testing was conducted using the "elmredict" function to form the test set. (4)

The accuracy of classification was then evaluated.

Among a total of 43 $Z_{s,i}$ indexes calculated for the poor cognition group, 34 were randomly selected for the training set and the remaining 9 were used as the testing set. Similarly, of the 55 $Z_{s,i}$ indexes in the excellent cognition group, 44 were randomly selected as the training set and the remaining 11 as

the testing set. In ELM, the type parameter was set as 1 (Set to 1 to solve the classification problem and set to 0 to solve the regression problem), the number of neurons in the hidden layer was set to 500, and the activation function TF was set to "sig" type. Then, the $Z_{s,i}$ indexes were trained and simulated using ELM. Finally, the classification accuracy for the elderly groups was assessed using the testing dataset.

2.4.3. N-fold cross-validation

In ELM, an N-fold cross-validation procedure was employed to test the accuracy of the algorithm as follows. The dataset was divided into N parts by setting $N-1$ parts as the training data and 1 part as the testing data. Thus, classification accuracy could be assessed for each procedure. The mean accuracy over N iterations (10 in this case) was utilized to estimate the accuracy of the algorithm.

3. Results

3.1. FC

The FC matrix diagrams constructed from the rs-fMRI data of elderly individuals with excellent cognitive test scores resembled those constructed from youth brains (Fig. 3). In contrast, the FC diagrams of the elderly group with poor cognitive test scores exhibited substantial connectivity differences compared with the excellent group between prefrontal lobe and middle frontal gyrus (AAL1–AAL7), within the temporoparietal region between the left Heschl's gyrus and the right inferior temporal gyrus (AAL79–AAL90), between the left superior parietal gyrus and the right inferior parietal gyrus (AAL59–AAL62), and within the occipital cortex between the left superior occipital lobe and the right inferior occipital lobe (AAL49–AAL54
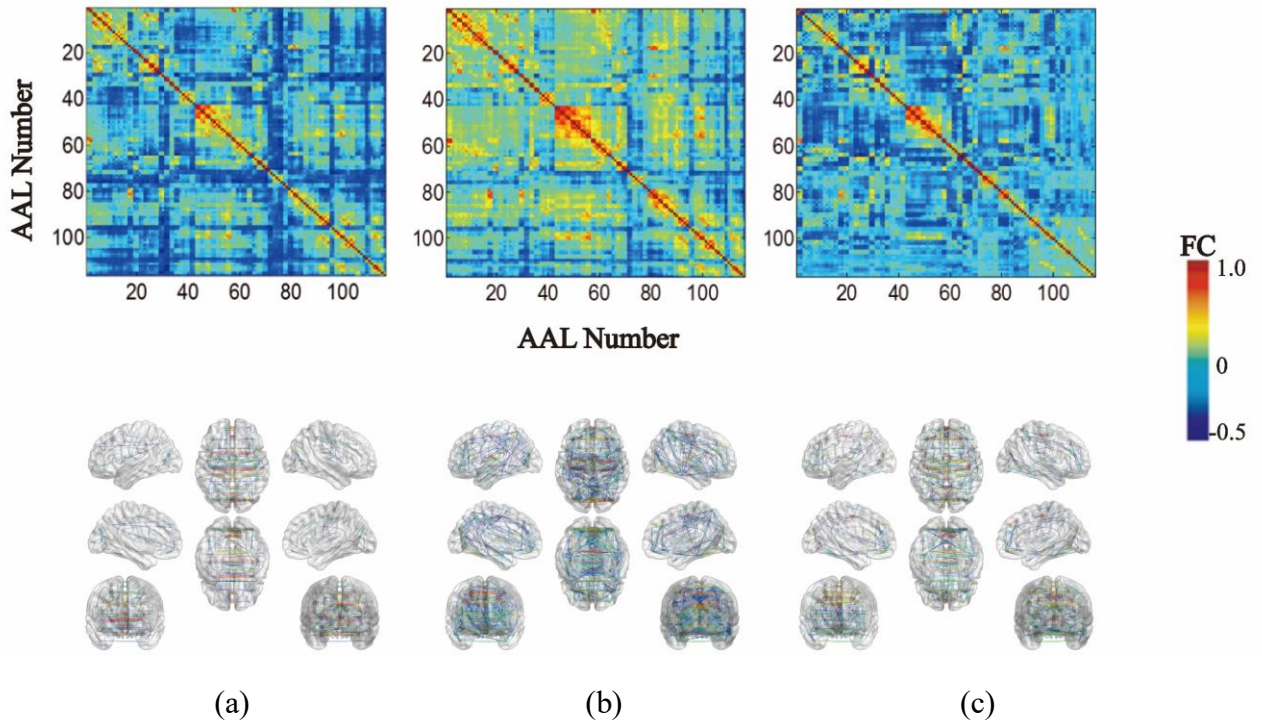

(a)   (b)   (c)

Fig. 3. Difference in whole-brain functional connectivity (FC) between elderly individuals with excellent and poor cognitive test performance. (a) Average FC values for the 55 old people with excellent cognitive scores. (b) Average FC values for the 43 old people with poor cognitive scores. (c) Average FC values for 90 healthy youth. The FC values are displayed as color-coded matrices in the upper panels and as BrainNet Viewer networks in the below panels. The middle red line in the matrix is the auto-

correlation(FC=1) for each region. Note the general resemblance between the excellent cognition group (left-most panel) and the young group (right-most panel), and the distinct FC map of the poor cognition group (middle panel).

3.2. *Functional biomarkers estimated using the fcMRI index model*

To identify regions most sensitive to cognitive test scores, scatter plots of fcMRI index differences between the two groups was constructed (Fig. 4a), which revealed five regions with significant differences (colored triangles): AAL60 (right superior parietal gyrus, Parietal_Sup_R), AAL83 (left superior temporal gyrus/temporal pole, Temporal_Pole_Sup_L), AAL1 (left precentral gyrus, Precentral_L), AAL59 (left superior parietal gyrus, Parietal_Sup_L), and AAL56 (right fusiform gyrus, Fusiform_R). These five brain areas (Fig. 4b) are therefore potential functional biomarkers (ROIs) for cognitive ability of healthy elderly. Indeed, ROC curves (Fig. 4c) suggested that each regional index distinguished poor from excellent cognitive performance. In addition, p values for all 5 regions were below 5% (Table 1). Thus, FC within subregions of the frontal, parietal, and temporal lobes can distinguish cognitive performance from the fcMRI indexes differences in the healthy elderly's brain.
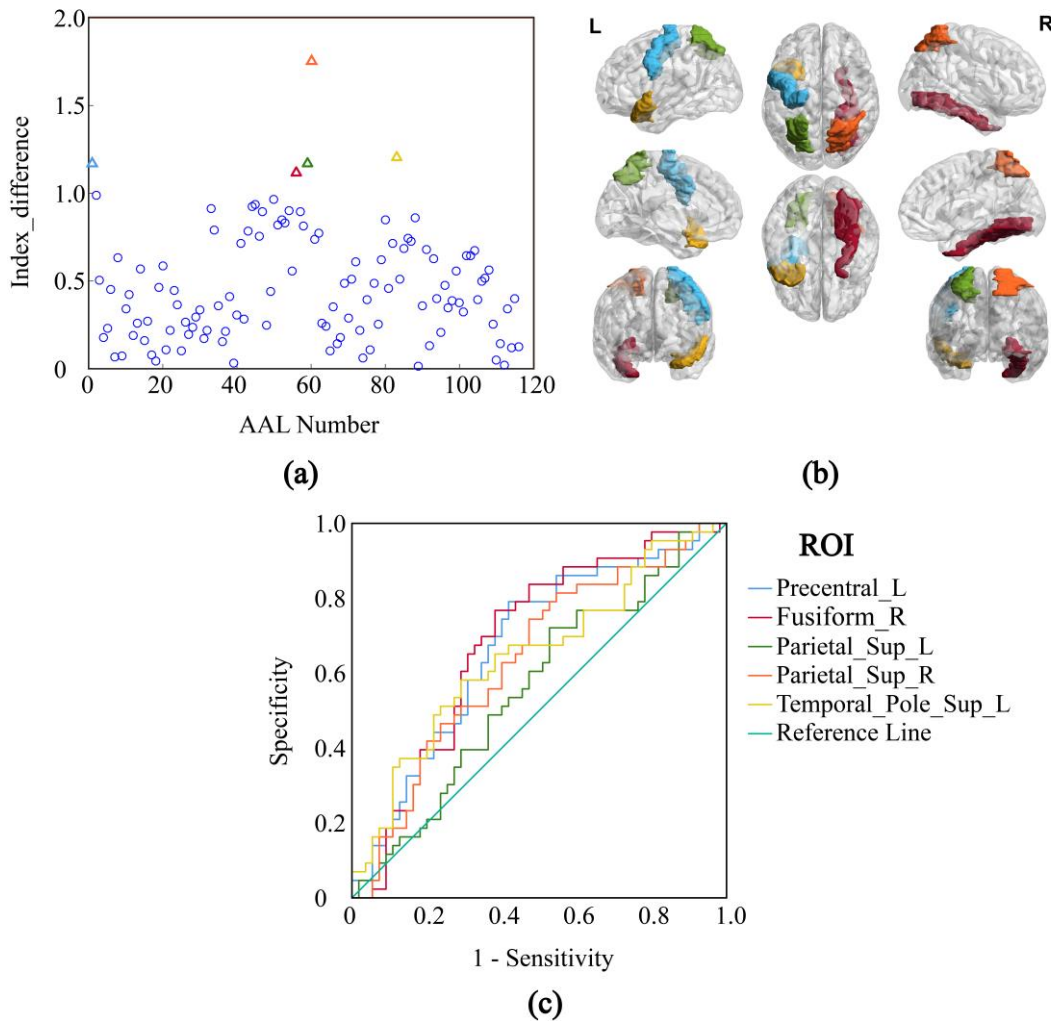

(a)

(b)

(c)

Fig. 4. Five brain regions of potential functional biomarkers of cognitive ability in healthy elderly. (a) Between-group differences in fcMRI index values for the whole brain. Regions with greatest significance are shown as colored triangles. Regions are specified according to the automatic anatomical labeling (AAL) atlas. (b) These same significant regions shown on a brain template using BrainNet Viewer. (c) ROC curves show that each region can distinguish poor from excellent cognitive ability among elderly individuals.

Table 1. The five brain areas showing the greatest differences in fcMRI indexes difference

AAL area	Significance (p-value, %)
AAL60 (Parietal_Sup_R)	0.1
AAL83 (Temporal_Pole_Sup_L)	0.2
AAL1 (Precentral_L)	0.2
AAL59 (Parietal_Sup_L)	0.5
AAL56 (Fusiform_R)	0.5

3.3. *Classification using the ELM model*

Of the 20 samples in the testing dataset (11 from the excellent cognition group and 9 from the poor group), 18 were correctly classified by the trained ELM model (90% accuracy) (Fig. 5), and the mean accuracy after N-fold cross-validation was 83.5% (Table 2).
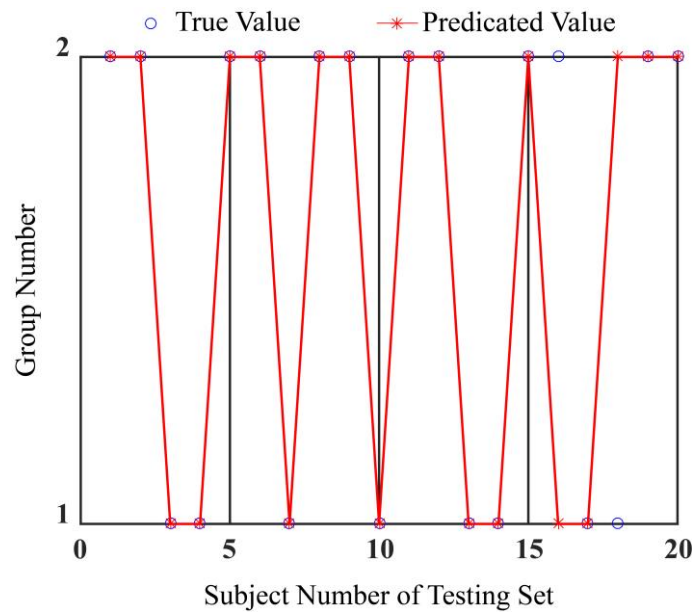

Fig. 5. Classification accuracy predicted by the trained extreme learning machine on the testing set. The excellent cognition group was denoted as Group Number 1, and the poor cognition group as Group Number 2. Overlap of a blue circle with a red asterisk indicates a correct classification. Of the 20 samples in the

testing set, 18 were correctly classified, thus classification accuracy was 90%.

Table 2 Classification accuracy (*CA*) tested by 10-fold cross-validation

N	CA (%)
1	85
2	80
3	85
4	85
5	85
6	80
7	90
8	80
9	85
10	80
Mean ± Std	**83.5 ± 3.3747**

4．Discussion

4.1． *Classification accuracy of the fcMRI index model at an individual level*

FC analysis is widely applied to localize dysfunctional brain areas at the group level. For example, Bettus et al. reported reduced FC among hippocampal structures in the hemisphere affected by seizures but increased FC among hippocampal structures in the healthy hemisphere [27]. Moreover, Fan et al. developed an FC model to identify significant relationships between cognitive test scores and individual FC values in the right frontal lobe, left hippocampus, right cingulate gyrus, and cerebellar posterior lobe in patients with cerebellar infarction [28]. In addition, the FC model developed by Egbert et al. revealed age-dependent effects on the associations between FC and cognitive functions in the resting state [29].

Our work extends such studies by demonstrating that FC differences associated with cognitive function are detectable among the healthy elderly at an individual level. Some of FC studies on predefined ROIs have found alterations within the frontal–parietal lobe network associated with memory, language skills, and attention as well as within the occipital neural network supporting visual processing[30], which is in accordance with the present findings. The functional biomarkers identified by our fcMRI index model also overlap with areas demonstrating structural abnormalities. For instance, using diffusion tensor imaging, Bolzenius et al. found that cognitive impairment was related to reduced structural integrity of the frontal

and temporal lobes [31]. Mokrisova et al. [32] also found impaired path integration associated with reduced hippocampal volume and thinning of the entorhinal and parietal cortices, suggesting that the neurodegeneration of the medial temporal lobe and parietal cortex are quantitative indicators of disease status. In contrast to studies with group level analysis, our fcMRI index model could distinguish excellent from poor cognition in healthy elderly individuals (Fig. 5 and Table 2).

4.2． *Greater sensitivity of the fcMRI index model compared with conventional FC models*

The fcMRI index model developed in this study identified FC changes in single brain areas able to distinguish excellent from poor cognition among healthy elderly individuals with 80%–90% accuracy, whereas conventional FC analysis (Fig. 3) using Pearson's coefficients could distinguish cognitive performance only at the group level. Furthermore, if the Pearson correlation matrices of two groups were considered as the feature vector inputs to the machine learning model, the highest classification accuracy achieved was only 72.2%. Similarly, Benesty et al. reported 71.43% accuracy using Pearson's correlation coefficients as FC metrics [33], and Goryawala et al. [34] found that neuropsychological scores and cortical volumes (temporal, parietal lobe, and cingulate gyrus) could distinguish early mild cognitive impairment (EMCI) from late mild cognitive impairment (LMCI) with 73.6% accuracy. Recently, Cheng et al. designed a new multi-modal and multi-task features-learning model to distinguish between EMCI and LMCI with 74.29% accuracy [35]. Thus, our fcMRI index model achieves substantially better classification accuracy among healthy elderly individuals with excellent or poor cognition than current classification models.

5． **Conclusions**

The fcMRI index model identified functional biomarkers sensitive to cognitive scores among healthy elderly individuals in the frontal, temporal, and parietal cortices. These biomarkers distinguished excellent from poor cognition with 83.5% accuracy. This FC index model may be useful for identifying additional biomarkers associated with cognitive function in healthy elderly individuals, thereby providing objective metrics for MCI prediction, monitoring, and treatment guidance.

Data Availability The data used in this article are from public data sets, and the source of the data is indicated in the article.

Code Availability The source of the software used in this article has been indicated in the article.

Compliance with Ethical Standards

Conflict of interest All authors declare that they have no conflict of interest.

Ethical Approval This study was approved by the Hebei University of Technology Ethics Committee.

Informed Consent This study was conducted in accordance with the Declaration of Helsinki. All participants received a thorough explanation of the experimental content in advance and gave their written consent for participation in the study.

References

1. Wu, Q., Chen, Y., Zhao, X., & Ming, D. (2019). A review of MRI based brain macro-micro structure change patterns. *Chinese J. Biomed. Eng, 38*(01), 94-101, doi:10.3969/j.issn.0258-8021.2019.01.012.

2. Chao, Y.-P., Wu, C. W., Lin, L.-J., Lai, C.-H., Wu, H.-Y., Hsu, A.-L., et al. (2020). Cognitive Load of Exercise Influences Cognition and Neuroplasticity of Healthy Elderly: An Exploratory Investigation. *Journal of Medical and Biological Engineering, 40*(3), 391-399, doi:10.1007/s40846-020-00522-x.

3. Santos, N. C., Costa, P. S., Cunha, P., Cotter, J., Sampaio, A., Zihl, J., et al. (2013). Mood is a key determinant of cognitive performance in community-dwelling older adults: a cross-sectional analysis. *AGE, 35*(5), 1983-1993, doi:10.1007/s11357-012-9482-y.

4. Santos, N. C., Costa, P. S., Cunha, P., Portugal-Nunes, C., Amorim, L., Cotter, J., et al. (2014). Clinical, physical and lifestyle variables and relationship with cognition and mood in aging: a cross-sectional analysis of distinct educational groups. *Frontiers in Aging Neuroscience, 6*, doi:10.3389/fnagi.2014.00021.

5. An, R., & Liu, G. G. (2016). Cognitive impairment and mortality among the oldest-old Chinese. *Int J Geriatr Psychiatry, 31*(12), 1345-1353, doi:10.1002/gps.4442.

6. Smart, C. M., Karr, J. E., Areshenkoff, C. N., Rabin, L. A., Hudon, C., Gates, N., et al. (2017). Non-Pharmacologic Interventions for Older Adults with Subjective Cognitive Decline: Systematic Review, Meta-Analysis, and Preliminary Recommendations. *Neuropsychology Review, 27*(3), 245-257, doi:10.1007/s11065-017-9342-8.

7. Braga, R. M., & Buckner, R. L. (2017). Parallel Interdigitated Distributed Networks within the Individual Estimated by Intrinsic Functional Connectivity. *Neuron, 95*(2), 457-471.e455, doi:10.1016/j.neuron.2017.06.038.

8. Yang, B.-H., Chen, J.-C., Chou, W.-H., Huang, W.-S., Fuh, J.-L., Liu, R. S., et al. (2020). Classification of Alzheimer's Disease from 18F-FDG and 11C-PiB PET Imaging Biomarkers Using Support Vector Machine. *Journal of Medical and Biological Engineering, 40*(4), 545-554, doi:10.1007/s40846-020-00548-1.

9. Cocchi, L., Zalesky, A., Fornito, A., & Mattingley, J. B. (2013). Dynamic cooperation and competition between brain systems during cognitive control. *Trends Cogn Sci, 17*(10), 493-501, doi:10.1016/j.tics.2013.08.006.

10. Zhang, D., & Raichle, M. E. (2010). Disease and the brain's dark energy. *Nat Rev Neurol, 6*(1), 15-28, doi:10.1038/nrneurol.2009.198.

11. Damaraju, E., Allen, E. A., Belger, A., Ford, J. M., McEwen, S., Mathalon, D. H., et al. (2014). Dynamic functional connectivity analysis reveals transient states of dysconnectivity in schizophrenia. *NeuroImage: Clinical, 5*, 298-308, doi:10.1016/j.nicl.2014.07.003.

12. Hutchison, R. M., Womelsdorf, T., Allen, E. A., Bandettini, P. A., Calhoun, V. D., Corbetta, M., et al. (2013). Dynamic functional connectivity: promise, issues, and interpretations. *Neuroimage, 80*, 360-378, doi:10.1016/j.neuroimage.2013.05.079.

13. Jiang, T. (2013). Brainnetome: a new -ome to understand the brain and its disorders. *Neuroimage, 80*, 263-272, doi:10.1016/j.neuroimage.2013.04.002.

14. Gallos, L. K., Makse, H. A., & Sigman, M. (2012). A

small world of weak ties provides optimal global integration of self-similar modules in functional brain networks. *Proc Natl Acad Sci U S A, 109*(8), 2825-2830, doi:10.1073/pnas.1106612109.

15. Biswal, B., Yetkin, Z., Haughton, V., & Hyde, J. (1995). Functional Connectivity in the Motor Cortex of Resting Human Brain Using Echo-Planar Mri. *Magnetic Resonance in Medicine, 34*, 537-541, doi:10.1002/mrm.1910340409.

16. Guerra-Carrillo, B., Mackey, A. P., & Bunge, S. A. (2014). Resting-state fMRI: a window into human brain plasticity. *Neuroscientist, 20*(5), 522-533, doi:10.1177/1073858414524442.

17. Meunier, D., Achard, S., Morcom, A., & Bullmore, E. (2009). Age-related changes in modular organization of human brain functional networks. *Neuroimage, 44*(3), 715-723, doi:10.1016/j.neuroimage.2008.09.062.

18. Shafto, M. A., & Tyler, L. K. (2014). Language in the aging brain: the network dynamics of cognitive decline and preservation. *Science, 346*(6209), 583-587, doi:10.1126/science.1254404.

19. Dua, M., Makhija, D., Manasa, P. Y. L., & Mishra, P. (2020). A CNN–RNN–LSTM Based Amalgamation for Alzheimer's Disease Detection. *Journal of Medical and Biological Engineering, 40*(5), 688-706, doi:10.1007/s40846-020-00556-1.

20. Cabral, J., Kringelbach, M., & Deco, G. (2017). Functional Connectivity dynamically evolves on multiple time-scales over a static Structural Connectome: Models and Mechanisms. *Neuroimage, 160*, doi:10.1016/j.neuroimage.2017.03.045.

21. Jenkinson, M., Beckmann, C. F., Behrens, T. E. J., Woolrich, M. W., & Smith, S. M. (2012). FSL. *Neuroimage, 62*(2), 782-790, doi:https://doi.org/10.1016/j.neuroimage.2011.09.015.

22. Jenkinson, M., Bannister, P., Brady, M., & Smith, S. (2002). Improved optimization for the robust and accurate linear registration and motion correction of brain images. *Neuroimage, 17*(2),

825-841, doi:10.1016/s1053-8119(02)91132-8.

23. Smith, S. M. (2002). Fast robust automated brain extraction. *Hum Brain Mapp, 17*(3), 143-155, doi:10.1002/hbm.10062.

24. Tzourio-Mazoyer, N., Landeau, B., Papathanassiou, D., Crivello, F., Etard, O., Delcroix, N., et al. (2002). Automated anatomical labeling of activations in SPM using a macroscopic anatomical parcellation of the MNI MRI single-subject brain. *Neuroimage, 15*(1), 273-289, doi:10.1006/nimg.2001.0978.

25. Hlinka, J., Palus, M., Vejmelka, M., Mantini, D., & Corbetta, M. (2011). Functional connectivity in resting-state fMRI: is linear correlation sufficient? *Neuroimage, 54*(3), 2218-2225, doi:10.1016/j.neuroimage.2010.08.042.

26. Xia, M., Wang, J., & He, Y. (2013). BrainNet Viewer: a network visualization tool for human brain connectomics. *PloS one, 8*(7), e68910-e68910, doi:10.1371/journal.pone.0068910.

27. Bettus, G., Guedj, E., Joyeux, F., Confort-Gouny, S., Soulier, E., Laguitton, V., et al. (2008). Decreased basal fMRI functional connectivity in epileptogenic networks and contralateral compensatory mechanism. *Hum Brain Mapp, 30*, 1580-1591.

28. Fan, L., Hu, J., Ma, W., Wang, D., Yao, Q., & Jingping, S. (2018). Altered baseline activity and connectivity associated with cognitive impairment following acute cerebellar infarction: A resting-state fMRI study. *Neurosci Lett, 692*, doi:10.1016/j.neulet.2018.11.007.

29. Egbert, A. R., Biswal, B., Karunakaran, K., Gohel, S., Pluta, A., Wolak, T., et al. (2018). Age and HIV effects on resting state of the brain in relationship to neurocognitive functioning. *Behav Brain Res, 344*, 20-27, doi:10.1016/j.bbr.2018.02.007.

30. Buckner, R. L., & DiNicola, L. M. (2019). The brain's default network: updated anatomy, physiology and evolving insights. *Nature Reviews Neuroscience, 20*(10), 593-608, doi:10.1038/s41583-019-0212-7.

31. Bolzenius, J. D., Laidlaw, D. H., Cabeen, R. P.,

Conturo, T. E., McMichael, A. R., Lane, E. M., et al. (2015). Brain structure and cognitive correlates of body mass index in healthy older adults. *Behav Brain Res, 278*, 342-347, doi:10.1016/j.bbr.2014.10.010.

32. Mokrisova, I., Laczo, J., Andel, R., Gazova, I., Vyhnalek, M., Nedelska, Z., et al. (2016). Real-space path integration is impaired in Alzheimer's disease and mild cognitive impairment. *Behav Brain Res, 307*, 150-158, doi:10.1016/j.bbr.2016.03.052.

33. Benesty, J., Chen, J., & Huang, Y. (2008). On the Importance of the Pearson Correlation Coefficient in Noise Reduction. *Audio, Speech, and Language Processing, IEEE Transactions on, 16*, 757-765, doi:10.1109/TASL.2008.919072.

34. Goryawala, M., Zhou, Q., Barker, W., Loewenstein, D. A., Duara, R., & Adjouadi, M. (2015). Inclusion of Neuropsychological Scores in Atrophy Models Improves Diagnostic Classification of Alzheimer's Disease and Mild Cognitive Impairment. *Comput Intell Neurosci, 2015*, 865265, doi:10.1155/2015/865265.

35. Cheng, N., Xiao, X., Hu, H., Yang, P., Wang, T., & Lei, B. (2019). Diagnosis of early mild cognitive impairment based on central automatic weighted multi task learning. *Chinese J. Biomed. Eng, 38*(06), 653-661, doi:10.3969/j.issn.0258-8021.2019.06.002.
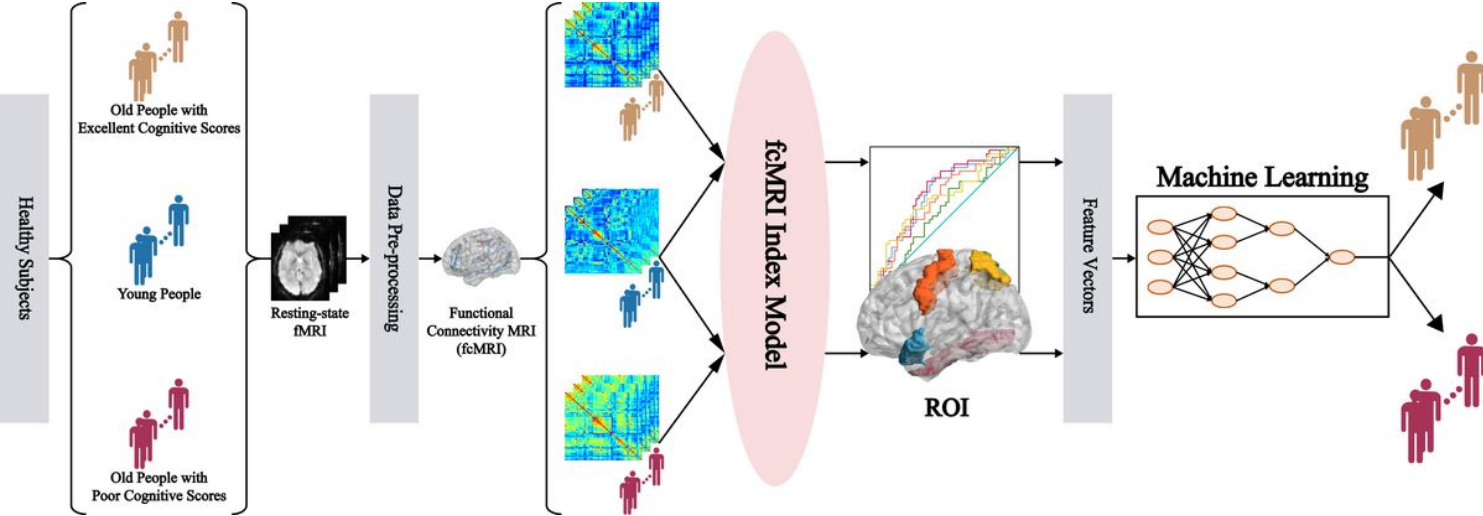
Figures

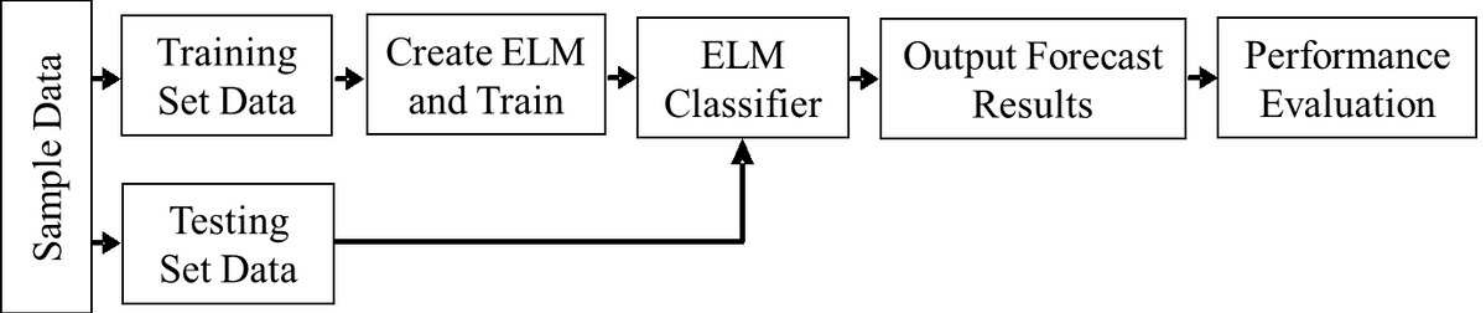**Figure 1**

Study flowchart

Figure 2

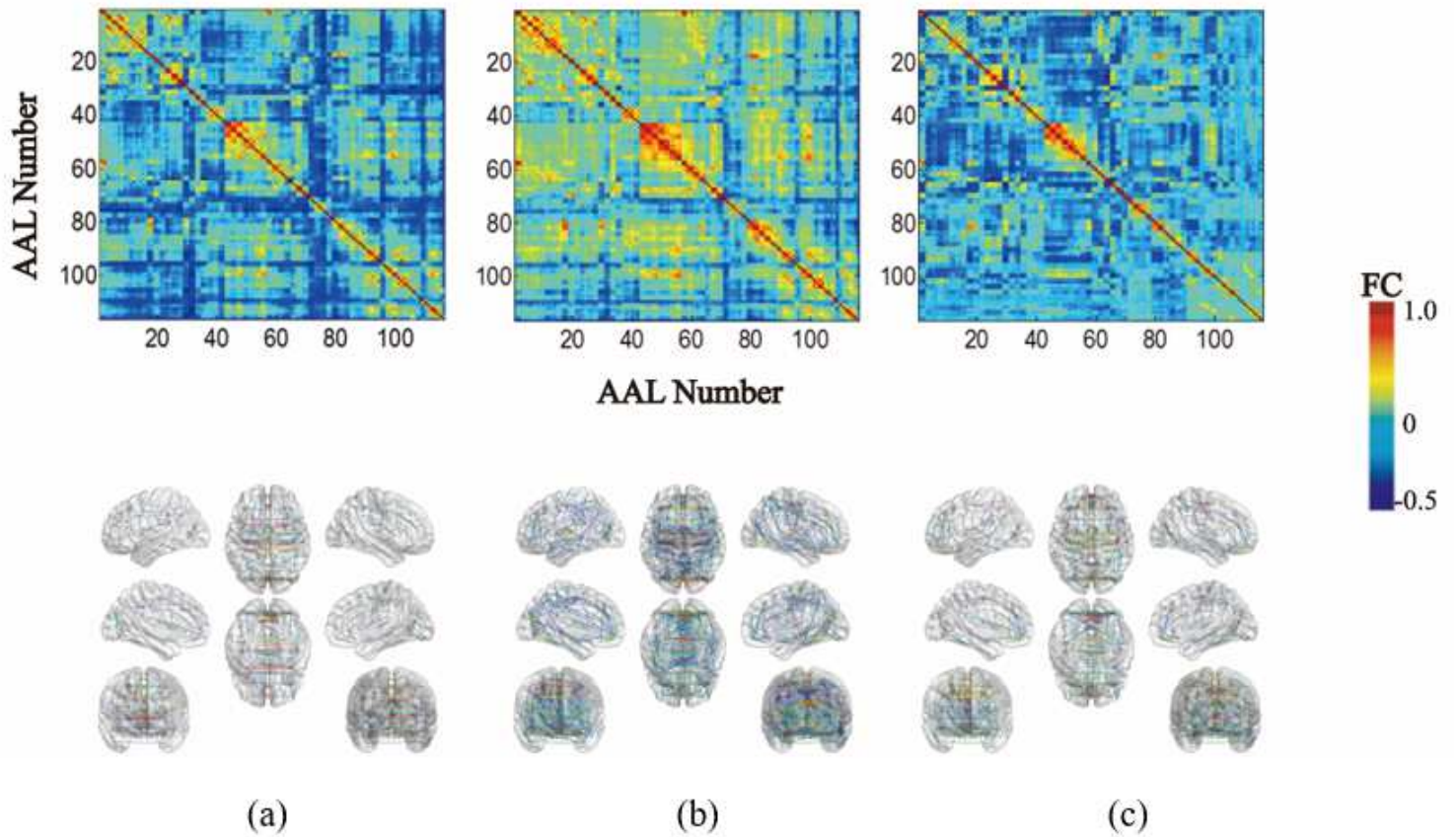Flowchart of extreme learning machine (ELM) classifier

Figure 3

Difference in whole-brain functional connectivity (FC) between elderly individuals with excellent and poor cognitive test performance. (a) Average FC values for the 55 old people with excellent cognitive scores. (b) Average FC values for the 43 old people with poor cognitive scores. (c) Average FC values for 90 healthy youth. The FC values are displayed as color-coded matrices in the upper panels and as BrainNet Viewer networks in the below panels. The middle red line in the matrix is the auto-correlation(FC=1) for each region. Note the general resemblance between the excellent cognition group (left-most panel) and the young group (right-most panel), and the distinct FC map of the poor cognition group (middle panel).
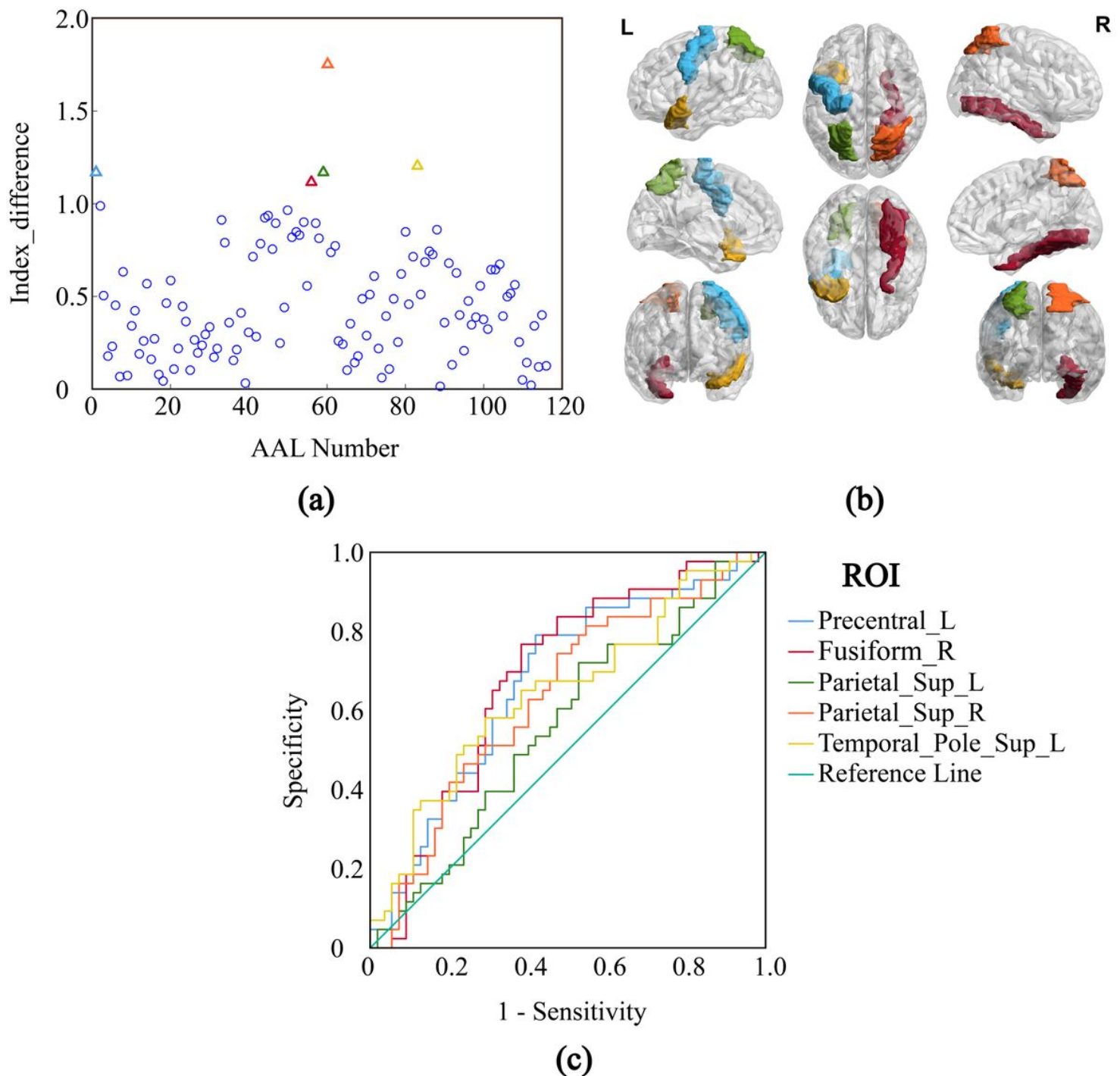
Figure 4

Five brain regions of potential functional biomarkers of cognitive ability in healthy elderly. (a) Between-group differences in fcMRI index values for the whole brain. Regions with greatest significance are shown as colored triangles. Regions are specified according to the automatic anatomical labeling (AAL) atlas. (b) These same significant regions shown on a brain template using BrainNet Viewer. (c) ROC curves show that each region can distinguish poor from excellent cognitive ability among elderly individuals.
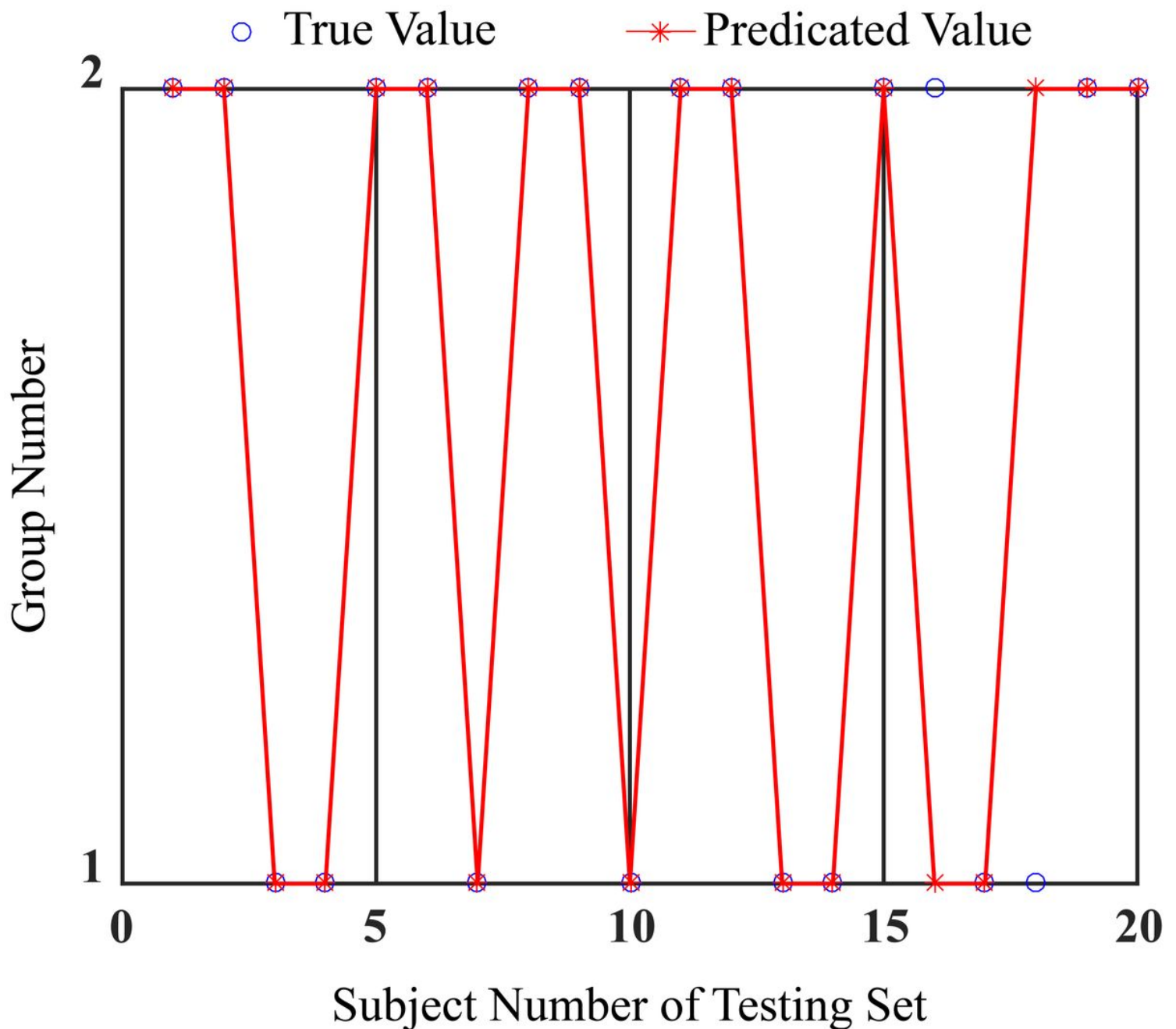
Figure 5

Classification accuracy predicted by the trained extreme learning machine on the testing set. The excellent cognition group was denoted as Group Number 1, and the poor cognition group as Group Number 2. Overlap of a blue circle with a red asterisk indicates a correct classification. Of the 20 samples in the testing set, 18 were correctly classified, thus classification accuracy was 90%.

Supplementary Files

This is a list of supplementary files associated with this preprint. Click to download.

- CoverLetter.pdf

- Highlight.docx